Time-Resolved WAXD and SAXS Investigations on Butyl Branched Alkane at Elevated Pressures

A. Rastogi,[†] J. K. Hobbs,[‡] and S. Rastogi*,[†]

Eindhoven Polymer Laboratories/Dutch Polymer Institute, Eindhoven University of Technology, P.O. Box 513, 5600 MB Eindhoven, The Netherlands, and University of Bristol, H. H. Wills Physics Laboratory, Tyndall Avenue, Bristol BS8 1TL, United Kingdom

Received November 29, 2001; Revised Manuscript Received April 22, 2002

ABSTRACT: The crystallization behavior and the morphological aspect of the butyl branched alkane $C_{96}H_{193}CH(C_4H_9)C_{94}H_{189}$ have been investigated using time-resolved wide-angle X-ray diffraction (WAXD) and small-angle X-ray scattering (SAXS) at atmospheric and elevated pressures. The solution crystallized sample shows pronounced crystalline reflections in WAXD with a lamellar thickness of 127 Å, corresponding to a once-folded structure in SAXS at atmospheric pressure. Cooling the sample from the melt at 4 °C/min at atmospheric pressure results in a lamellar thickness of 104 Å with chains having a tilt angle of 35°. The crystallization of the branched alkane at pressures of ca. 4 kbar and the same cooling rate of 4 °C/min reveals a new crystal reflection emerging between the (100) monoclinic and the (110) orthorhombic reflections. Simultaneous to the appearance of the new reflection, a sudden shift in the Bragg *d* value of the (110) orthorhombic reflection occurs, indicating densification of the orthorhombic unit cell. The new reflection has been assigned as the pseudohexagonal phase attributed to the crystallization of the butyl branches at elevated pressures. The pseudohexagonal phase merged into the orthorhombic phase upon releasing pressure and reappeared on increasing pressure. Compared to lamellar thickness at atmospheric pressure, an increased lamellar thickness of 118 Å was observed at ca. 4 kbar with SAXS.

1. Introduction

Ultralong *n*-alkanes with monodisperse nature serve as model systems to study the fundamentals of polymer behavior. To probe the chain folding in polymers, the synthesis of pure *n*-paraffins, with typical chain lengths between 100 and 400 C atoms, was carried out by Whiting et al.[1] These long *n*-alkanes proved to be an immense asset for understanding the crystallization process in polymers with linear chains. More recently, in addition to larger quantities of the linear materials, two other branched *n*-alkanes were synthesized by Brooke et al.:[2] $C_{96}H_{193}CH(R)C_{94}H_{189}$ where R = CH_3 and $CH_3(CH_2)_3$. The branched alkane allows us to obtain a direct insight into the role played by the side branches during the crystallization process and serves as a potential model system for polyethylene copolymers.

Detailed SAXS studies on these linear and branched *n*-alkanes have been performed by Ungar et al.[3−9] under isothermal and/or nonisothermal conditions at atmospheric pressure. The investigations unveil and explain the complex chain-folding process during crystallization. In situ SAXS experiments using synchrotron radiation make it possible to follow the crystallization process. It was observed that the crystals formed in the early stages of crystallization have lamellae with the thickness of a noninteger fraction (NIF) of the extended form. This transient form soon transforms into an integer form, either via thickening (to extended form) or thinning (to once-folded form F2). In the past few years, Ungar et al. have elucidated the structure and mechanism of the formation of the NIF form using SAXS (including electron density profiles), Raman longitudinal acoustic modes (LAM) spectroscopy, and differential scanning calorimetry (DSC).

A comparative study of the crystallization mechanism of the linear and branched alkane[7] done earlier indicated that, in the sequence melt → NIF → F2, the melt → NIF step is fast but the NIF → F2 step is slow in linear alkanes. The crystallization mechanism is understood in the following manner. In a NIF lamella of a linear alkane a half-crystallized molecule generally has two cilia. During crystallization, neither of the two cilia is long enough to make a complete adjacent reentry, provided no rearrangements in the already crystallized part occur. This retards the formation of F2 crystals. However, the reverse is true for the branched alkane. Isothermal crystallization study of the methyl branched alkane $C_{96}H_{193}CH(CH_3)C_{94}H_{189}$ revealed that the high rate of NIF → F2 transition is attributed to the fact that here the only successful deposition mode of the first stem (first half) of the molecule is the one which places the branch at a lamellar basal surface and the chain end at the opposite surface of the same lamella. The other half of the molecule (uncrystallized cilium) is then ideally suited to complete a second traverse of the crystal.[7]

To have a better insight into the crystallization mechanism and resulting crystal structures of the branched alkanes with respect to the branch length, in this paper pressure−temperature studies have been performed. Complementing the studies done earlier, the phase behavior of the butyl branched alkane $C_{96}H_{193}CH(C_4H_9)C_{94}H_{189}$ has been investigated at elevated pressures. The current paper addresses the significant

† Eindhoven University of Technology.
‡ University of Bristol.
* To whom correspondence should be addressed.

10.1021/ma012078l CCC: $22.00
Published on Web 06/12/2002

part played by the butyl branches during the entire crystallization process at elevated pressures and also how it influences the crystal lattice in general. Variations in the crystal structure have been followed in situ with WAXD while the morphological aspects have been investigated using in situ SAXS. The two scattering techniques summed together provide a comprehensive analysis of the crystallization behavior of the branched alkane containing four carbon atoms as a side chain.

2. Experimental Section

2.1. Materials. The meticulous synthesis of the butyl branched alkane $C_{96}H_{193}(C_4H_9)C_{94}H_{189}$ has been done by Brooke et al.[2] The structure of the branched alkane is well-defined in terms of the distribution of the side branch and its monodisperse nature. The butyl ($-C_4H_9-$) branch lies exactly after 96 C atoms and thereafter followed by 94 C atoms. If we envisage the folding of a single molecule, then the branch lies almost in the middle of the fold. Synthesis of the sample occurs in solution, and the sample is recovered in the form of precipitate. After washing and drying, the sample is used for experimentation. Thus, the as-received sample will be termed as a solution crystallized sample.

2.2. Equipment. The high-pressure measurements were done using a piston−cylinder type pressure cell, similar to the one designed by Hikosaka and Seto.[10] The maximum attainable pressure in the current setup is 5 kbar. The temperature can be varied from room temperature to 300 °C. A sample of 0.4 mm thickness is placed in between the two diamond windows, each having a thickness of 1 mm and surrounded by Teflon spacer rings. The use of diamond windows enables the performance of in situ X-ray diffraction studies.

In situ wide-angle X-ray diffraction measurements were performed using monochromatic X-rays of wavelength 0.718 Å and the high flux available on the beamline ID11-BL2 at the European Synchrotron Radiation Facility (ESRF), Grenoble, France. The lower wavelength was required to reduce X-ray absorption by the diamond windows. Each diffraction pattern was exposed for 25 s on a two-dimensional CCD detector, and two frames were recorded every minute. The data were corrected for curvature of the detector using the diffraction pattern of a specific calibration grid placed in the X-ray beam. The circle coordinates of strong reflections were used to determine the correct beam center. The two-dimensional X-ray patterns were transformed into one-dimensional plots by performing integration along the azimuthal angle using the FIT2D program of Dr. Hammersley of ESRF.

Time-resolved SAXS experiments were performed using a wavelength of 1 Å in the beamline ID02 at ESRF, Grenoble. The detector used was an image intensifier coupled to a Frelon CCD camera. Pixel array dimensions were 1024 × 1024. The exposure time for each pattern was approximately 1 s, and the delay time was adjusted to record 2 frames/min. The average long spacing was calibrated using orders from a standard specimen of Silver Behenate. A sample-to-detector distance of 3 and 5 m was used, the latter in order to get better resolution in terms of the *d* values.

A Linkam THMS600 hot stage was used to perform heating and cooling scans at atmospheric pressure. The sample was filled in a glass capillary and fixed with the help of a holder on the hotstage, mounted perpendicular to the X-ray beam to enable in situ SAXS measurements.

3. Results and Discussion

Figure 1 shows a cycle adopted for the experiments. The sequence of paths together formulate a specific pressure−temperature cycle, to which the sample is exposed. In the present paper results on WAXD are reported first followed by SAXS results to give further insight into the morphological changes. Before performing studies at the elevated pressures and temperatures, to have an insight into the crystal structure and morphological features, X-ray studies were carried out at atmospheric pressure.

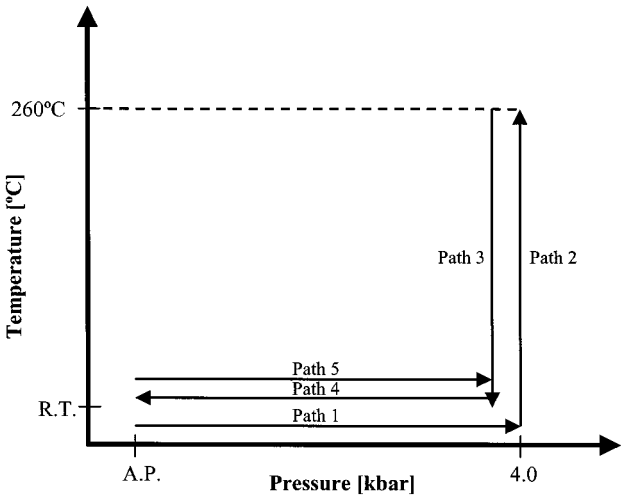

Figure 1. Pressure−temperature cycle showing the paths to which the butyl branched alkane is exposed. Pressure is gradually increased at room temperature (RT, 25 °C) to 4 kbar along path 1 followed by heating until melting (path 2). The sample is cooled at 4 °C/min to room temperature at constant elevated pressure (path 3) after which the pressure is released subsequently to atmospheric pressure (AP) (path 4). To observe the changes in the phase behavior of the pressure-crystallized sample (i.e., the sample exposed to the paths 1−4), pressure is again increased along path 5 at room temperature.

3.1. Crystal Structure and Morphological Features of Butyl Branched Alkane at Atmospheric Pressure. (a) WAXD. Figure 2a shows a two-dimensional (2D) WAXD pattern of a solution-crystallized butyl branched alkane in between the diamond windows, at atmospheric pressure and room temperature. The pattern shows orthorhombic and monoclinic crystalline reflections. The appearance of monoclinic reflections is a result of shear[11] that occurs during sampling process in the pressure cell. The innermost ring depicts the (100) monoclinic reflection followed by the strong (110) orthorhombic reflection. The other less intense reflections are (200) monoclinic and (200) orthorhombic reflections. The outermost reflection is relatively weak and is assigned to the (−201) monoclinic phase. It is observed that the *d* value for the (110) orthorhombic reflection ($d_{110ortho} = 4.08$ Å) is similar to that of linear paraffins or linear polyethylene reported in the literature[12] ($d = 4.11$ Å). This suggests that the orthorhombic packing is maintained; however, the side branches resort to the lamellar surface. The lattice spacing for the monoclinic phase is $d_{100mono} = 4.53$ Å.

(b) SAXS. The SAXS pattern of the solution-crystallized butyl branched alkane depicted in Figure 2b shows three sharp orders. The first-order reflection at 127 Å is representative of the fact that the chains are once folded (F2) and correspond to a regular stacking of the lamellae having chains without any tilt. The *d* value justifies that the solution-crystallized sample has vertically stacked once-folded chains with the butyl branches in the middle of the fold contributing to the long spacing. The second and third orders at 61 and 40 Å are the harmonics of the first order. To an approximation,[13] the values agree well with the theoretically calculated long spacing [{(95 + 4) × 1.272} + 2 = 127.9 Å for the first order, 63.9 Å for the second order, and 42.6 Å for the

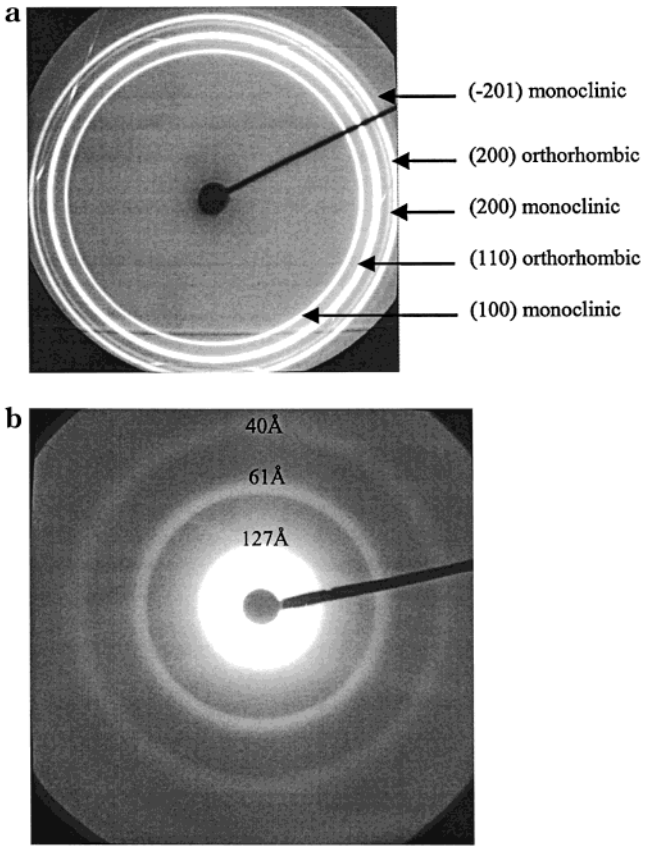

Figure 2. (a) 2-D wide-angle X-ray diffractogram of butyl branched alkane placed in between the diamond windows, showing crystalline orthorhombic and monoclinic reflections under ambient conditions (AP and RT). The lines observed across the pattern are from the diamond windows. (b) 2-D SAXS pattern showing three sharp orders in the solution-crystallized butyl branched alkane.

third order] without considering the tilt. These calculations are in accordance with Ungar et al.[6]

Before examining the behavior of the alkane at elevated pressures, heating and cooling experiments in a Linkam hot stage were performed at atmospheric pressure, and morphological changes were studied using time-resolved SAXS. The alkane was heated at 4 °C/min at atmospheric pressure. The changes in the lamellar thickness are followed in situ. Figure 3a shows Lorentz-corrected intensity $I(q)q^2$ vs "q" plot, where "q" is the scattering vector. The three orders at 127, 61, and 40 Å show a gradual splitting into two parts with increasing temperature. A fraction of the old order (127, 61, and 40 Å) is retained and weakens, while the other part intensifies and gradually moves toward higher "q" values. The overall intensity of the reflections stays constant. The new positions for the other part of the first, second, and third orders just before melting are approximately 108, 53, and 35 Å, respectively. These d values correspond well to a lamella having F2 chain structure with a chain tilt angle of approximately 35°. Since these reflections are observed below the melting temperature, the changes in SAXS patterns on heating are attributed to the occurrence of chain tilt, where chain tilt within the lamellae is associated with minimization of the surface free energy.[14−16] The reflections disappear upon complete melting at 125 °C.

Figure 3b shows the SAXS pattern recorded in situ while the sample was cooled at 4 °C/min from melt at atmospheric pressure. The first-order reflection appears

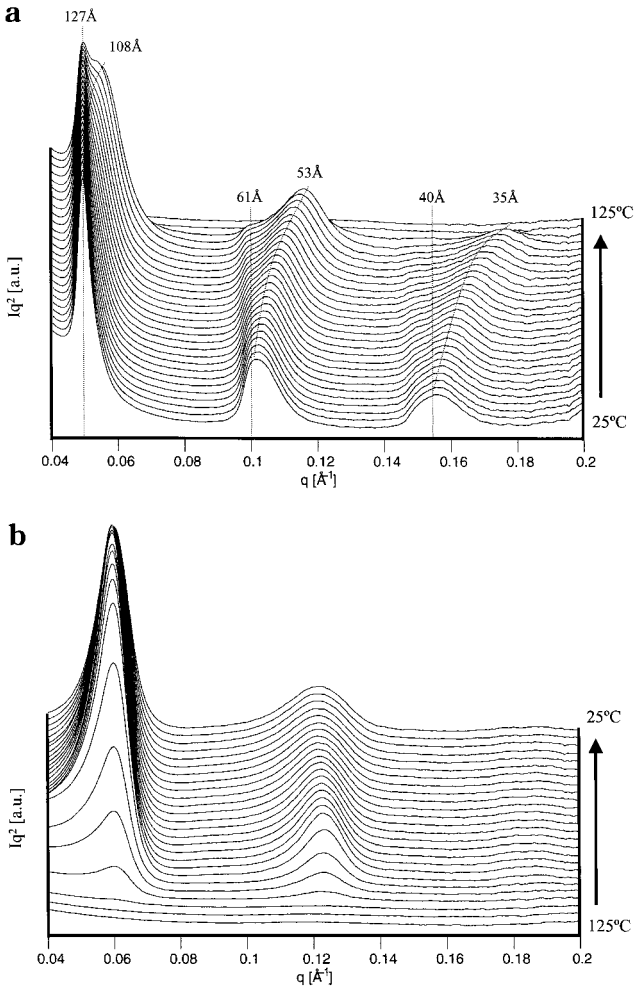

Figure 3. (a) Integrated SAXS patterns showing Lorentz corrected intensity Iq^2 vs q plot during heating at 4 °C/min at atmospheric pressure. The three orders at 127, 61, and 40 Å show a gradual shift to higher "q" values with increasing temperature. (b) In situ recorded SAXS patterns indicate that first-order and second-order reflections appear at 104 and 51 Å, respectively, during cooling at 4 °C/min at atmospheric pressure. X-ray wavelength used 1.0 Å.

at 104 Å, which is different to the position of the first order in the solution-crystallized sample, i.e., 127 Å. This long spacing is approximately equal to the expected value of the once-folded chains with tilt angle of 35° [{(99 × 1.272) + 2} cos 35° = 104.8 Å]. The second order is at 51.0 Å. This indicates that the crystallization from the melt starts with a tilted chain structure within the lamellae. The chains within the crystal show tilt at an angle of 35° from the very early stages of crystallization while the tilted structure is retained upon further cooling to room temperature. There was no observation of the noninteger folds when the sample was cooled at a rate of 4 °C/min, at atmospheric pressure. This suggests that during nonisothermal crystallization chains tend to resort to the once-folded structure with the butyl branch on the lamellar surface.

3.2. In Situ Structure and Morphological Studies at Elevated Pressures and Temperature. In situ high-pressure WAXD and SAXS studies were done at the beamlines ID11/BL2 and ID02, respectively, at the European Synchrotron Radiation Facility in Grenoble, France. Experiments have been performed along the pressure−temperature paths shown in Figure 1. The paths adopted enable a broader understanding of the

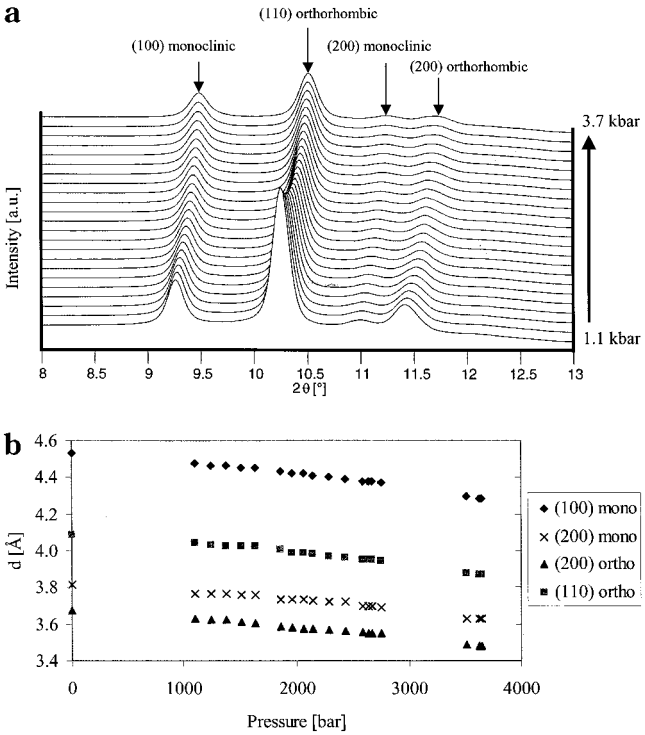

Figure 4. (a) 3-D plot of integrated WAXD patterns during pressure increase at room temperature (25 °C). (b) Plot of Bragg *d* values (interplanar spacing) of crystal reflections vs pressure increase at room temperature, showing compression of the crystalline lattices at elevated pressures. X-ray wavelength used 0.718 Å.

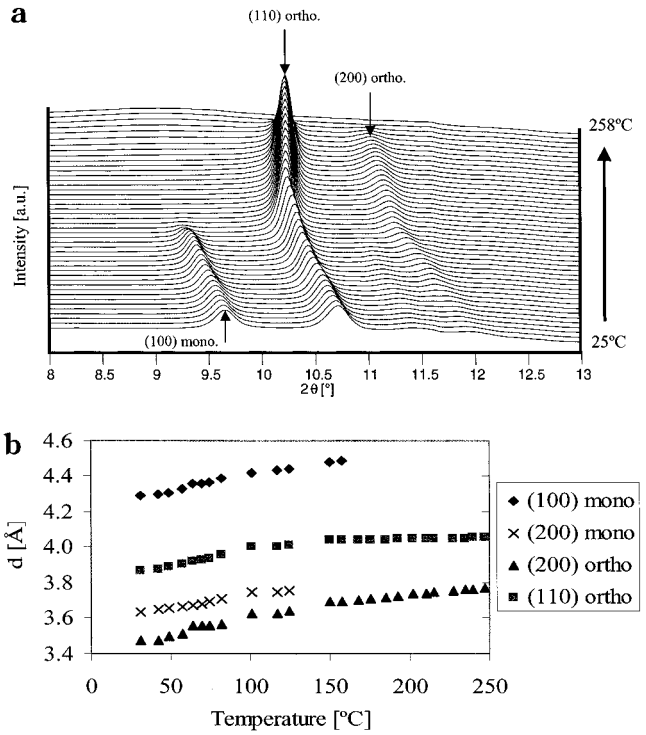

Figure 5. (a) Time-resolved WAXD patterns during heating at 4 °C/min at 3.8 kbar along path 2. The (100) monoclinic and the (110) orthorhombic reflections gradually shift to lower 2θ value, where the former disappears at ca. 160 °C followed by an increase in the intensity of the orthorhombic reflection. The reflections vanish on melting at ca. 258 °C. (b) Bragg *d* values of the crystalline reflections plotted as a function of temperature during heating at 3.8 kbar. The initial slope of the curves suggests thermal expansion of the compressed crystalline lattices upon heating. X-ray wavelength used 0.718 Å.

structure and morphology of the butyl branched alkane. The experimental observations along these paths are discussed below.

3.2.1. Path 1. Increasing Pressure at Room Temperature. The WAXD pattern of a butyl branched alkane in between the diamond windows showed pronounced orthorhombic and monoclinic reflections at atmospheric pressure, depicted earlier in Figure 2a. The intensity of all reflections decreases because of a decrease in the sample thickness due to compression as shown in Figure 4a. The reflections move toward higher angles with subsequent increase of pressure. Figure 4b shows that increasing pressure leads to a compression of the crystalline lattice, resulting in lower *d* values (interplanar spacing). The change in the Bragg *d* value of the (110) orthorhombic reflection from 4.08 Å at atmospheric pressure to 3.87 Å at ca. 3.7 kbar confirms the same. At a pressure of nearly 3.7 kbar, intensity of all the reflections decreases. However, the two relatively intense reflections of orthorhombic and monoclinic crystals (i.e., (110) orthorhombic and (100) monoclinic) are more visible compared to the other reflections that become less pronounced on the same intensity scale. Conversely, in situ SAXS performed on the solution-crystallized alkane along path 1 did not reveal any major changes in the lamellar thickness. The first- and second-order reflections at 127 and 61 Å remain unaltered.

3.2.2. Path 2. Heating at 4 °C/min at a Fixed Pressure of 3.8 kbar. On heating, isobarically at ca. 3.8 kbar, Figure 5a shows that the orthorhombic and monoclinic reflections tend to shift toward lower angles, implying a thermal expansion of the compressed crystalline lattice with increasing temperature. The (100) monoclinic reflection vanishes at approximately 160 °C with a slight increase in intensity of the (110) orthorhombic reflection. The increase in the intensity indicates transformation of monoclinic crystals to the orthorhombic phase. Since the monoclinic phase is associated with the presence of shear in the crystals, its disappearance at ca. 160 °C suggests removal of shear within the crystals. On further heating, no significant shift in the (110) reflection is observed, as evident from the slope (*d*/temperature) in Figure 5b. The orthorhombic reflections diminish as the sample melts at ca. 258 °C. The shifts in (110) and (200) reflections on heating are in agreement with the expansion of the crystalline lattice.

The SAXS observations along path 2 (as indicated in Figure 1) are similar to those observed during heating the solution-crystallized sample at atmospheric pressure. The first-order reflection shifts from lower to higher angles and moves from 127 to approximately 104 Å (*d* value corresponding to a once-folded structure with a chain tilt angle of 35°). The shift in the *d* value on heating is again associated with tilt in the chains within the crystal, as explained above.

3.2.3. Path 3. Cooling at 4 °C/min at a Fixed Pressure of 4 kbar. (a) WAXD. Figure 6a illustrates the crystallization process and the changes occurring in the crystal structure during cooling at 4 °C/min at a fixed pressure of nearly 4 kbar. Upon crystallizing from the melt, crystal formation occurs directly in the orthorhombic phase. The orthorhombic (110) and (200) reflections gain intensity with increasing supercooling. A weak monoclinic reflection appears at ca. 148 °C. With subsequent cooling at ca. 70 °C, a relatively broad and

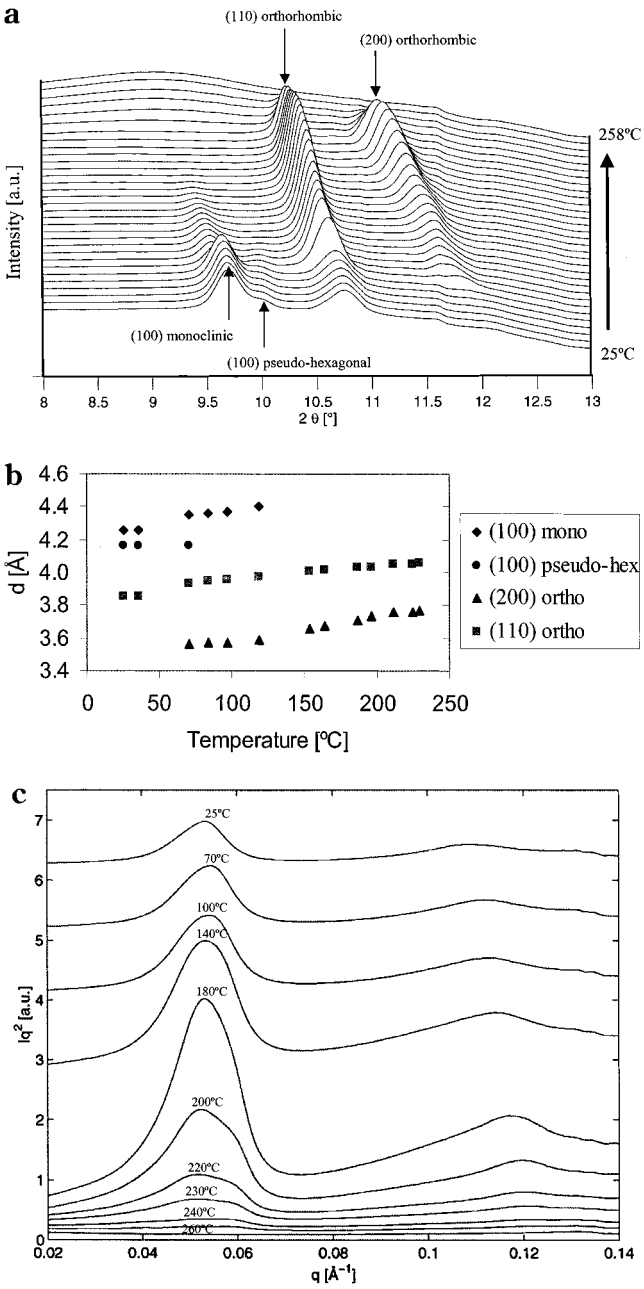

Figure 6. (a) Crystallization of butyl branched alkane at elevated pressures of 4.0 kbar is depicted with a series of integrated WAXD patterns recorded while cooling at a rate of 4 °C/min. The orthorhombic (110) and (200) reflections appear first which gain intensity with increasing supercooling. A weak (100) monoclinic reflection appears at ca. 148 °C. Upon further cooling at ca. 70 °C, sudden drop in the intensity of the (110) orthorhombic reflection is observed with the appearance of a new reflection and a simultaneous increase in the intensity of (100) monoclinic reflection. Considering the position of the new reflection (d = 4.16 Å) between the (100) monoclinic and (110) orthorhombic reflection, it has been termed a "pseudo-hexagonal" phase. (b) Plot of Bragg d values of various crystalline reflections vs temperature during cooling at elevated pressure of 4.0 kbar, along path 3. (c) Time-resolved SAXS patterns recorded during cooling at a rate of 4 °C/min at 3.8 kbar show a relatively broad first-order reflection at 118 Å and a second-order reflection at 58 Å. An overall drop in SAXS intensity follows on cooling. X-ray wavelength used for WAXD 0.718 Å and for SAXS 1.0 Å.

weak new reflection appears next to the monoclinic reflection. On appearance of the new reflection a sudden drop in the intensity of the orthorhombic reflection and a simultaneous increase in the intensity of the monoclinic reflection are observed. The presence of the new reflection becomes more evident with cooling. The (110) and (200) orthorhombic peaks show a sudden shift to higher angles, implying a decrease in the d value (d = 3.85 and 3.58 Å, respectively) with the concomitant incoming of the new reflection. The new position of the (110) and (200) reflections suggests a contracted state of the orthorhombic crystalline lattice in the branched paraffin at ca. 4 kbar. Moreover, the new relatively weak reflection persists at 4.16 Å, adjacent to the monoclinic reflection at 4.26 Å as illustrated in Figure 6b.

In terms of the Bragg d value, the position of the new reflection is fairly close to the (100) reflection for the hexagonal packing in linear polyethylene (see Figure 6b). In linear polyethylene, for the hexagonal (columnar/condis phase) unit cell,[12] a = 8.46 Å, b = 4.88 Å, and c = 2.45 Å, and the Bragg $d_{100\text{hex}}$ is at 4.22 Å. Considering position of the new reflection (4.16 Å) between the (110) reflection (3.85 Å) for the orthorhombic phase and the monoclinic reflection (4.26 Å), and the higher symmetry for the hexagonal packing, the new reflection can be assigned as the (100) reflection for the columnar like pseudohexagonal phase.[17] Definite assignment of a phase to the new reflection is not straightforward as only one reflection is observed.

At room temperature, the new positions of the orthorhombic (110) and (200) reflections for the branched alkane (at 3.85 and 3.58 Å. respectively) indicate strongly a compressed lattice when compared to *n*-alkane or linear polyethylene at atmospheric pressure. The latter has unit cell dimensions a = 7.4 Å, b = 4.94 Å, and c = 2.55 Å, where d = 4.11 and 3.70 Å for the (110) and (200) reflections, respectively. The remarkable changes that are observed with the incoming of the new reflection need to be summarized: (a) a sudden shift in the (110) and (200) reflections as described above; (b) a drop in the intensity of the (110) and (200) reflections of the orthorhombic phase followed by (c) a simultaneous increase in intensity of the monoclinic reflection. The sudden shift in reflections, as mentioned above (a), becomes more evident when the experiments are performed along path 4 and path 5, depicted in Figure 1.

To have insight into the morphological changes with the incoming of the new reflection, SAXS experiments along path 3 have been also performed, i.e., cooling from the melt at 4 °C/min at ca. 4 kbar, under conditions similar to WAXD described above.

(b) SAXS. Figure 6c shows the SAXS patterns recorded during cooling from the melt at 4 °C/min at a pressure of nearly 4 kbar. A shoulder is observed at approximately 108 Å during the initial stages of crystallization (within the temperature region 245−220 °C) that seems to disappear as the SAXS peak intensifies at d = 118 Å. A first-order reflection evolves at 118 Å while a second-order reflection is observed at approximately 58 Å. The position of the first order is slightly greater than that for the once-folded (F2) structure having a chain tilt angle of 35° within the crystal and less than that for the structure without the chain tilt. Several *possible* explanations can be suggested that may account for such a d value. First, the d value at 118 Å obtained on cooling can be a result of the presence of two different populations, i.e., crystals having tilted chains and/or crystals having chains without tilt. Since no discrete reflection at 127 Å

resulting from lamellae without chain tilt is observed, it is preferable not to consider chains without tilt within the lamellae.

In view of WAXD results, another explanation could be the presence of different tilt angles for the chains in the monoclinic or orthorhombic phases, where the former appears on cooling. Since the monoclinic reflection in WAXD patterns is observed below 100 °C (approximately) and no shift in SAXS peak (118 Å) is observed, neither any new reflection is observed near 100 °C, the possible second explanation, suggested here, is unlikely.

A third explanation for the increase in the *d* value could be due to the ordering of the side chains from the interface of the two contiguous lamellae, resulting in a pseudohexagonal phase as observed in WAXD. This may also explain the observed drop in intensity on cooling in the SAXS pattern. Hence, the drop in intensity can be due to decrease in the electron density fluctuation between the crystalline and amorphous regions, with crystallization of the amorphous regions in the pseudohexagonal phase. Considering the new reflection, which comes up in WAXD at ca. 70 °C, no new order was seen corresponding to that new reflection in SAXS. This indicates that the crystals formed at that temperature due to the crystallization of the side branches are not regular enough to cause a jump in the crystal–amorphous electron density profile. They are unable to break the limited long period.

3.2.4. Path 4. Releasing Pressure at Room Temperature. (a) WAXD. The presence of the pseudohexagonal phase is realized to a greater extent when pressure is released from 3.8 kbar to atmospheric pressure at room temperature along path 4 in Figure 1. The position of the pseudohexagonal reflection remains the same while the (110) orthorhombic and (100) monoclinic reflections move subsequently to lower angles, as shown in Figure 7a. The shift in the reflection seems to be mainly due to lattice expansion with the release of pressure. The monoclinic reflection disappears at ca. 2 kbar. Because of the shift in the orthorhombic (110) reflection to higher *d* values, the hexagonal reflection gets merged into the orthorhombic reflection. Thereafter, an increase in the intensity of the (110) and (200) orthorhombic reflections is observed. Figure 7b explicitly shows the shift in the *d* values of the various crystalline reflections upon releasing pressure. It is to be noted that while the reflections associated with other crystalline lattices like orthorhombic and monoclinic move to higher *d* values, the *d* value for the pseudohexagonal phase remains constant. From the observations summarized above, it may be concluded that the butyl branches, which tend to lie within the amorphous domains on the crystal surface, most likely lead to the formation of the pseudohexagonal phase. Finally, at room temperature and atmospheric pressure, only the orthorhombic phase is observed, and no monoclinic reflections are present.

(b) SAXS. Figure 7c shows that when the pressure is released at room temperature, the first-order shifts from ca. 118 to 110 Å. Similarly, there is a shift in the second order from approximately 58 to 54 Å. The change in the *d* value may be a result of the change in the tilt and/or possibly due to the loss of ordering of the side chains, reasoning in line with the explanation given under section 3.2.3. In addition to the observed shift in the *d* values the overall SAXS intensity increases on releasing pressure within a range of 200 bar in the vicinity of 2.5 kbar. When combined with the WAXD measurements, the sudden increase in the intensity is in the regime when monoclinic crystals disappear with the pseudohexagonal phase. The increase in SAXS intensity is associated with an increase in overall

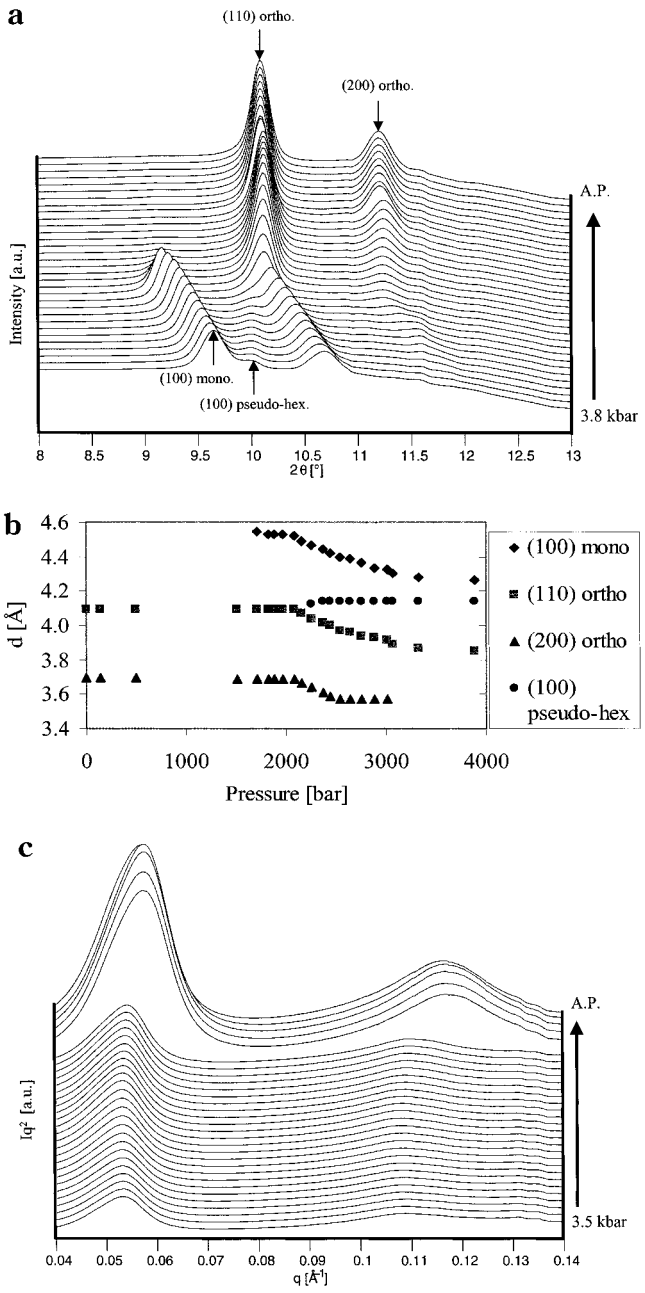

Figure 7. (a) 3-D WAXD plot shows that, upon releasing pressure at room temperature, (100) monoclinic and (110) orthorhombic reflections move to lower angles while the (100) pseudohexagonal reflection stays at the same position. The latter finally merges in the (110) orthorhombic reflection, resulting in an overall increase in the intensity of the orthorhombic reflections. (b) The *d* values for the various crystalline reflections are plotted against pressure. Upon releasing pressure at room temperature along path 4, the *d* value of the (110) orthorhombic reflection increases from 3.85 to 4.08 Å while the $d_{100hex} = 4.16$ Å merges with that of the (110) orthorhombic reflection at ca. 2 kbar. At atmospheric pressure the *d* values for the various crystalline reflections attain values similar to those in linear paraffins. (c) Series of SAXS pattern depicting a gradual shift in the first order from 118 Å at ca. 3.5 kbar to 110 Å at atmospheric pressure during pressure release. The second-order shifts from 58 to 54 Å. Also, an overall increase in the SAXS intensity occurs.

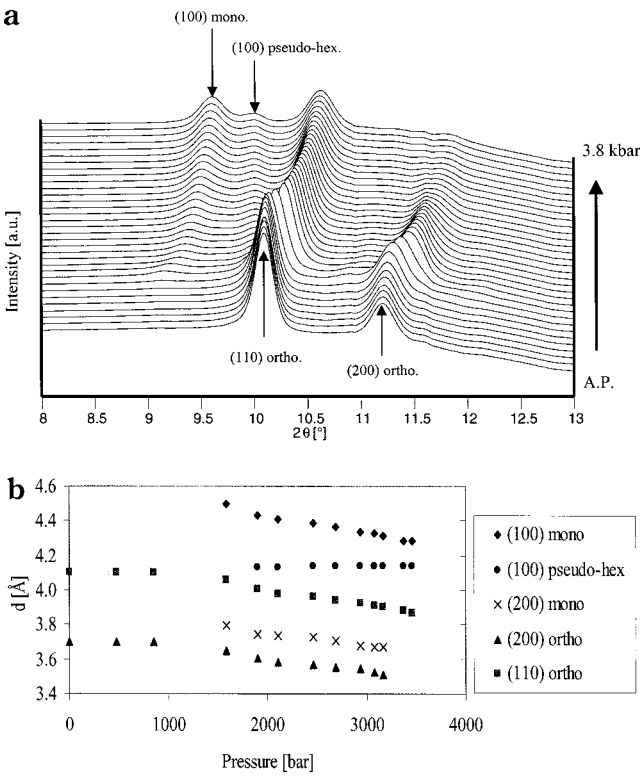

Figure 8. (a) In situ recorded WAXD patterns during pressure increase along path 5, showing the reappearance of the new reflection assigned to the pseudohexagonal phase at ca. 2.0 kbar. (b) Plot of Bragg *d* values vs pressure depicting the variation in the crystalline reflections consequent to pressure increase along path 5 and appearance of the pseudohexagonal phase. The $d_{110ortho}$ (4.08 Å) moves to a lower value (3.85 Å) simultaneous to the appearance of the (100) pseudohexagonal phase at 4.16 Å. X-ray wavelength used 0.718 Å.

electron density fluctuation between the crystalline and amorphous components. In our case such an increase in the electron density fluctuation can occur because of the transition of the earlier crystalline butyl branches into the amorphous phase with releasing pressure. To further strengthen the hypothesis, experiments have been performed along path 5 with increasing pressure.

3.2.5. Path 5. Increasing Pressure Again at Room Temperature. The intensity of orthorhombic (110) and (200) reflections decreases as the crystals transform into the monoclinic phase with increasing pressure as shown in Figure 8a. At ca. 1.8 kbar, a reflection appears, having the same intensity and peak profile at a *d* value 4.16 Å similar to that in Figure 7a. Because of its similarity to the new reflection indicated in Figure 7a, this reflection can again be assigned as pseudohexagonal. A shift simultaneous with the appearance of the new reflection in the *d* values of (110) and (200) orthorhombic reflections to a lower spacing is observed. The final *d* values for these reflections, shown in Figure 8b, once again correspond to very dense crystalline packing. The appearance and disappearance of the pseudohexagonal reflection can be associated with the regular stacking of butyl branches within the amorphous zone of the orderly stacked crystalline layers. The reflection becomes evident with the compression of the butyl branches, resulting in columnar hexagonal packing. The concomitant appearance of the pseudohexagonal reflection with the monoclinic phase suggests a possibility of transformation of part of the crystal to the monoclinic phase.

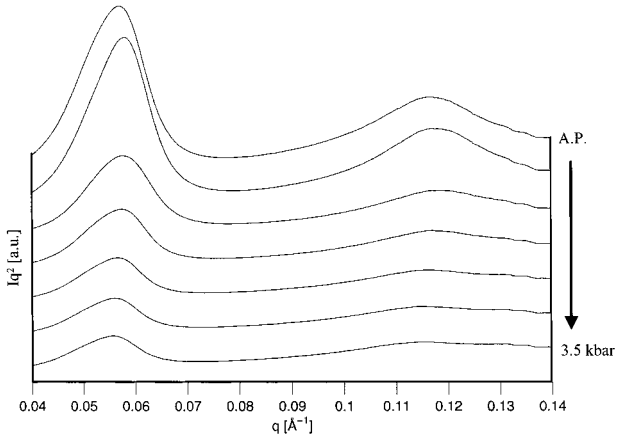

Figure 9. SAXS patterns showing an overall decrease in the intensity at ca. 1.8 kbar and a shift in the first order from 110 to 118 Å upon pressure increase at room temperature along path 5. X-ray wavelength used 1.0 Å.

SAXS follows a similar recovery of the features observed earlier on releasing pressure. For example, Figure 9 shows a sudden decrease in overall intensity within the vicinity of 2 kbar on increasing pressure and a shift in *d* value from 110 to 118 Å (at 3.5 kbar). When combined with WAXD, the sudden changes observed in SAXS appear with the incoming of the pseudohexagonal phase together with the monoclinic phase. The drop in SAXS intensity on increasing pressure can be explained in the same way as the increase in intensity on releasing pressure.

Keeping the crystallization conditions imposed on the sample in perspective, in contrast to the starting material (solution-crystallized alkane), a new pseudohexagonal phase appeared between the (110) orthorhombic and the (100) monoclinic reflections in the pressure-crystallized sample, i.e., the sample that has been exposed along path 1 to path 4, shown in Figure 1.

The overall experimental observations strongly support the following hypothesis. To minimize the free energy during crystallization, the butyl side groups would tend to occupy the lamellar basal surface, thereby contributing to the amorphous regions of the crystal. The formation of a new phase concomitant with the shift in the lattice spacing of the orthorhombic reflection indicates that there is a densification of the orthorhombic unit cell. The sudden densification or contraction of the unit cell is a consequence of the severe stress forces transferred due to the crystallization of the butyl branches. A sufficiently high supercooling enables the relatively short butyl branches to form a high-symmetry molecular ordering. To accommodate these short branches, less dense molecular packing is essential. The fact is realized by favoring columnar hexagonal[17] packing of these short branches. The phase is called a "pseudohexagonal" phase here, a phase having a high symmetry. The overall phenomenon of sudden densification of the unit cell with the appearance of a new phase indicates that it is a result of the simultaneous crystallization and densification of two different parts of the same crystal. The new phase arising due to the crystallization of the butyl branches results in densification of the already existing orthorhombic unit cell. The new reflection was not observed in other linear alkanes or the methyl branched alkane when exposed to a cycle similar to that depicted in Figure 1. This suggests that, as expected, the methyl

units were too short to organize and thus could not form a separate phase.

4. Conclusions

The crystallization behavior of $C_{96}H_{193}CH(C_4H_9)$-$C_{94}H_{189}$ has been investigated using in situ WAXD and SAXS at elevated pressures (up to 4 kbar). At atmospheric pressure and room temperature, the WAXD pattern shows prominent orthorhombic and monoclinic reflections. The SAXS pattern exhibits a regularly stacked lamella of the solution-crystallized alkane with a lamellar thickness corresponding to the straight once-folded chains without a tilt. A gradual tilting of the chains is observed upon heating the sample at 4 °C/min. Cooling at the same rate results in lamellae having a tilted chain structure (tilt angle of 35°) with no order seen for the regular straight chain structure. No non-integer fold was observed during cooling at 4 °C/min at atmospheric pressure, suggesting a strong drive for the chains to adopt a once-folded structure where the branches tend to lie on the lamellar surface.

The orthorhombic and monoclinic crystal lattices contract upon increasing pressure at room temperature with no change in lamellar thickness. An increase in the *d* values of the orthorhombic and monoclinic reflections is observed due to thermal expansion of the unit cell during heating at elevated pressures of ca. 3.8 kbar. SAXS patterns show the tilting of the chains during heating. WAXD patterns show an incoming of a new reflection on cooling at approximately 70 °C at elevated pressures (3.8 kbar). This reflection is attributed to the crystallization of the butyl branches and has been termed a "pseudohexagonal" phase. It has a *d* value of 4.16 Å, which is in proximity to the *d* value of the hexagonal phase observed in linear polyethylene. A concomitant shift to lower *d* values in the orthorhombic reflections with the appearance of this phase indicates a sudden densification of the unit cell resulting in a compressed orthorhombic crystal lattice, thus leading to the drop in SAXS intensity. An increased lamellar thickness of 118 Å compared to 104 Å at atmospheric pressure is realized at room temperature after cooling at 4 °C/min under ca. 4 kbar. The "pseudohexagonal" phase observed in WAXD disappears as it merges into the orthorhombic reflection upon releasing pressure. The new phase becomes more evident when it reappears on increasing pressure. The simultaneous appearance of the "pseudohexagonal" phase and the contraction of the orthorhombic unit cell give a strong indication that this new reflection is part of the same crystal arising due to the crystallization of the butyl branches lying on the crystal basal surface. A relatively broad and weak reflection of the pseudohexagonal phase is in accordance with the small crystal size of butyl branches, where these crystals at high pressures are formed from the amorphous domains that exist between the crystalline regions so observed at atmospheric pressure.

Acknowledgment. We thank the EPSRC and Dr. G. M. Brooke for providing the alkanes used in this work. We are also thankful to the European Synchrotron Radiation Facility (ESRF), Grenoble, France, for the X-ray measurements and specially Dr. Ann Terry (ESRF, ID11/BL2) and Dr. Volker Urban (ID02) for their help during the experiments. We also extend our thanks to Bob van der Gender and Frank van der Burgt for their help during experiments.

References and Notes

(1) Bidd, I.; Whiting, M. C. *J. Chem. Soc., Chem. Commun.* **1985**, 543.
(2) Brooke, G. M.; Burnett, S.; Mohammed, S.; Proctor, D.; Whiting, M. C. *J. Chem. Soc., Perkin Trans. 1* **1996**, 1635.
(3) Ungar, G.; Stejny, J.; Keller, A.; Bidd, I.; Whiting, M. C. *Science* **1985**, 229.
(4) Ungar, G.; Keller, A. *Polymer* **1986**, *27*, 1835.
(5) Organ, S. J.; Keller, A.; Hikosaka, M.; Ungar, G. *Polymer* **1996**, *37*, 2517.
(6) Zeng, X.; Ungar, G. *Polymer* **1998**, *39*, 4523.
(7) Ungar, G.; Zeng, X.; Brooke, G. M.; Mohammed, S. *Macromolecules* **1998**, *31*, 1875.
(8) Zeng, X.; Ungar, G. *Macromolecules* **1999**, *32*, 3543.
(9) Spells, S. J.; Zeng, X.; Ungar, G. *Polymer* **2000**, *41*, 8775.
(10) Hikosaka, M.; Seto, T. *Jpn. J. Appl. Phys.* **1982**, *21*, L332.
(11) Hay, I. L.; Keller, A. *J. Polym. Sci., Part C* **1970**, *30*, 289.
(12) Mark, J. E. *Physical Properties of Polymers Handbook*; AIP Press: New York, 1996; Chapter 30, p 410.
(13) We have made an approximate calculation for the lamellar thickness taking 95 as an average of 96 C atoms on one side and 94 C atoms on the other side of the 4 C atoms branch in the butyl branched alkane. Since 4 C atoms are relatively small to have gauche defects, we have considered the trans−trans configuration with the 4 C atoms protruding out of the basal plane of a lamella. The addendum 2 in the formula takes into account the radii of the H atoms from CH_3 groups present at the end of a chain.
(14) Ungar, G.; Zeng, X. *Chem. Rev.* **2001**, *101*, 4157.
(15) Sullivan, P. K.; Weeks, J. J. *J. Res. Natl. Bur. Stand., Sect. A* **1970**, *74*, 203.
(16) Gautam, S.; Balijepalli, S.; Rutledge, G. C. *Macromolecules* **2000**, *33*, 9136.
(17) Ungar, G. *Polymer* **1993**, *34*, 2050.

MA012078L